

RESEARCH

Open Access



RNA-Seq transcriptomic analysis with Bag2D software identifies key pathways enhancing lipid yield in a high lipid-producing mutant of the non-model green alga *Dunaliella tertiolecta*

Lina Yao¹, Tin Wee Tan², Yi-Kai Ng¹, Kenneth Hon Kim Ban^{2,3}, Hui Shen¹, Huixin Lin¹ and Yuan Kun Lee^{1*}

Abstract

Background: For many years, increasing demands for fossil fuels have met with limited supply. As a potential substitute and renewable source of biofuel feedstock, microalgae have received significant attention. However, few of the current algal species produce high lipid yields to be commercially viable. To discover more high yielding strains, next-generation sequencing technology is used to elucidate lipid synthetic pathways and energy metabolism involved in lipid yield. When subjected to manipulation by genetic and metabolic engineering, enhancement of such pathways may further enhance lipid yield.

Results: In this study, transcriptome profiling of a random insertional mutant with enhanced lipid production generated from a non-model marine microalga *Dunaliella tertiolecta* is presented. D9 mutant has a lipid yield that is 2- to 4-fold higher than that of wild type. Using novel Bag2D-workflow scripts developed and reported here, the non-redundant transcripts from *de novo* assembly were annotated based on the best hits in five model microalgae, namely *Chlamydomonas reinhardtii*, *Coccomyxa subellipsoidea* C-169, *Ostreococcus lucimarinus*, *Volvox carteri*, *Chlorella variabilis* NC64A and a high plant species *Arabidopsis thaliana*. The assembled contigs (~181 Mb) includes 481,381 contigs, covering 10,185 genes. Pathway analysis showed that a pathway from inositol phosphate metabolism to fatty acid biosynthesis is the most significantly correlated with higher lipid yield in this mutant.

Conclusions: Herein, we described a pipeline to analyze RNA-Seq data without pre-existing transcriptomic information. The draft transcriptome of *D. tertiolecta* was constructed and annotated, which offered useful information for characterizing high lipid-producing mutants. *D. tertiolecta* mutant was generated with an enhanced photosynthetic efficiency and lipid production. RNA-Seq data of the mutant and wild type were compared, providing biological insights into the expression patterns of contigs associated with energy metabolism and carbon flow pathways. Comparison of *D. tertiolecta* genes with homologs of five other green algae and a model high plant species can facilitate the annotation of *D. tertiolecta* and lead to a more complete annotation of its sequence database, thus laying the groundwork for optimization of lipid production pathways based on genetic manipulation.

Keywords: *Dunaliella tertiolecta*, Next-generation sequencing, RNA-Seq, Random insertional mutant, Lipid metabolism

*Correspondence: yuan_kun_lee@nuhs.edu.sg

¹ Department of Microbiology and Immunology, Yong Loo Lin School of Medicine, National University of Singapore, Singapore, Singapore
Full list of author information is available at the end of the article

Background

After the oil crises of the 1970s and 1980s, much of the debate about world oil markets centered on the limitations of supply [1]. Alternative fuels become highly demanding. The changes in the overall fuel market environment have led to focus on reassessing long-term trends in liquid fuels markets, such as natural gas plant liquids, biofuels, gas-to-liquids, coal-to-liquids, kerogen (i.e., oil shale) and refinery gain [1]. As an alternative and renewable source of lipid-rich biomass feedstock for biofuels, microalgae have been explored and received considerable attention in the recent years [2]. These microorganisms are able to use the solar energy to combine water with carbon dioxide which is the main component of greenhouse gas emissions to produce biomass [3], which convert sunlight into chemical energy in the form of reduced carbon molecules (carbohydrates, oils/fats). Oils or triacylglycerols (TAGs) can be used directly or by a simple chemical conversion to fatty acid methyl esters as biodiesels [4].

Over the past few decades, several thousand algae and cyanobacteria species have been screened for high lipid content, of which several hundred oleaginous species have been isolated and characterized under laboratory and/or outdoor culture conditions [2]. Among them, *Dunaliella tertiolecta* is considered one of the most promising species. *D. tertiolecta* is a flagellated unicellular marine microalga that belongs to the Chlorophyta phylum. The rationale for selecting *D. tertiolecta* in this study lies in its ability to produce large quantities of lipids (up to 67 % of organism dry weight), a high tolerance to salt, temperature and light, rapid growth rate in hyper saline environments which eliminate contaminations from the pure cultures, utilize inorganic nutrients present in salt-water, wastewater or brackish water along with sunlight to produce biomass using CO₂ as a carbon source through photosynthesis, and it lacks a rigid cell wall which eases product extraction and genetic manipulation [5–10].

Genetic manipulation is a common strategy for enhancement of lipid overproduction in microalgae to channel metabolites to lipid biosynthesis by overexpressing one or more key enzymes in microalgal strains [11]. The understanding of pathways and crucial enzymes is essential to modify microalgal strains. To perform gene manipulation in microalgal strains, their genome information is necessary. Currently, few complete genome sequences of microalgae are available, such as green microalgae *Chlamydomonas reinhardtii*, *Coccomyxa subellipsoidea* C-169, *Ostreococcus lucimarinus*, *Volvox carter* and *Chlorella variabilis* NC64A [12–16]. However, few of these algae are ideal producers of lipids, and, as such, extensive bioinformatics studies and genetic modifications on other species are needed. Enlarged

data analytical capability and improved downstream processing in the NGS technology have been developed in recent years [9, 17, 18], such as the studies to identify and construct lipid and starch biosynthesis and catabolism pathways in the microalga *D. tertiolecta* [9], which applied NGS-based transcriptomics to species without reference genome sequences. Although Hamid et al. [9] provided a good approach to investigating into the transcriptome and annotating partial transcripts, the incomplete nuclear and chloroplast genome sequences of *D. tertiolecta* limited the global transcriptomics studies on RNA-Seq data.

In this study, a *D. tertiolecta* mutant D9 with enhanced lipid production was generated. An in-house program was developed using BLASTX algorithms by comparing with five green algal lineages and one high plant species to construct the draft transcriptomic database of *D. tertiolecta* for RNA-Seq analysis and further target gene manipulation. RNA-Seq analysis elucidated the regulation of lipid synthetic pathways in the D9 mutant.

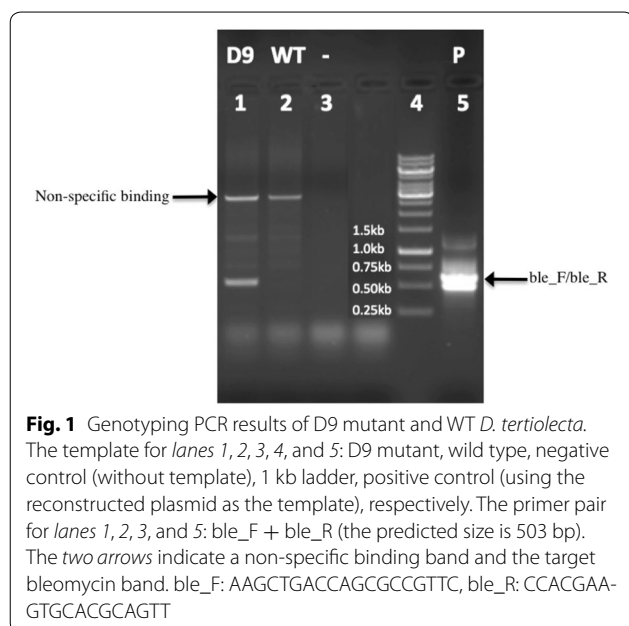
Results and discussions

Mutant selection and physiological characterization

Mutants of *D. tertiolecta* subjected to random insertional mutagenesis were generated by transformation using pGreenII0000 plasmid with a bleomycin selection cassette. Zeocin-resistant transformants were screened on 0.08 M ATCC medium agar plates with zeocin. About 30 mutants resistant to zeocin were selected. One transformant with constantly enhanced lipid production was selected and named D9 for further characterization. The bleomycin transgene was detected through genotyping PCR (Fig. 1).

Growth kinetics of the D9 and wild-type *D. tertiolecta* cells grown at 0.5 M ATCC medium were examined and shown in Fig. 2a. In comparison with the wild type, D9 shared the similar growth kinetics. Neutral lipids in D9 was examined and compared with that in the wild type. As shown in Fig. 2d, the D9 mutant produced neutral lipids at the late exponential and early stationary phases at about 2- to 4-fold of that in the wild type, indicating that some carbon flow channeling may be occurring. As an attempt to use a rapid fatty acid detection protocol, we also compared the quantification results obtained from the GC-MS analysis with those obtained from Nile red assays. The Nile red data showed a good correlation with the GC-MS data ($R^2 = 0.86$, Additional file 1), indicating such an assay could potentially be used as a high-throughput screen for identifying the next generation of fatty acid-overproducing mutant strains, which was also tested and suggested by Peng Xu [19].

Photosynthetic activities (including rates of photosynthesis, photosynthetic efficiency and the maximum



photochemical capacity) of the D9 and wild-type *D. tertiolecta* cells were investigated. D9 mutant in general showed increased photosynthetic performance (Fig. 2b, c), with around twofold increase in photosynthetic efficiency compared to that of wild-type *D. tertiolecta*.

The glycerol production and starch content of D9 and wild-type cells at stationary phase were investigated. Regardless of the neutral lipids production and photosynthetic performance, glycerol production and starch contents in the two genotypes were comparable, as shown in Fig. 2e, f. Lipids and starch are known as endogenous carbon storage compounds [20], and glycerol is the osmo-regulator for *Dunaliella* [21]. The enhanced photosynthetic efficiency resulted in a carbon flux to lipid synthesis and accumulation, rather than starch or glycerol production.

Pre-analysis and de novo assembly of sequenced data

The RNA-Seq data analysis workflow for the non-model species used in this study is illustrated in Fig. 3, which includes upstream cell culturing, harvest and downstream data interpretation steps.

The paired-end reads (130 bps in length/read) from each library were generated using Illumina MiSeq Sequencer. The short paired-end reads from D9, WT were pooled and examined with pre-alignment QA/QC and a secondary pre-alignment QA/QC after trimming was subsequently used. QA/QC reports mentioned throughout the paper are presented in Table 1. The trimmed *D. tertiolecta* short paired-reads were merged and subjected to the assembly programs, Velvet and Oases.

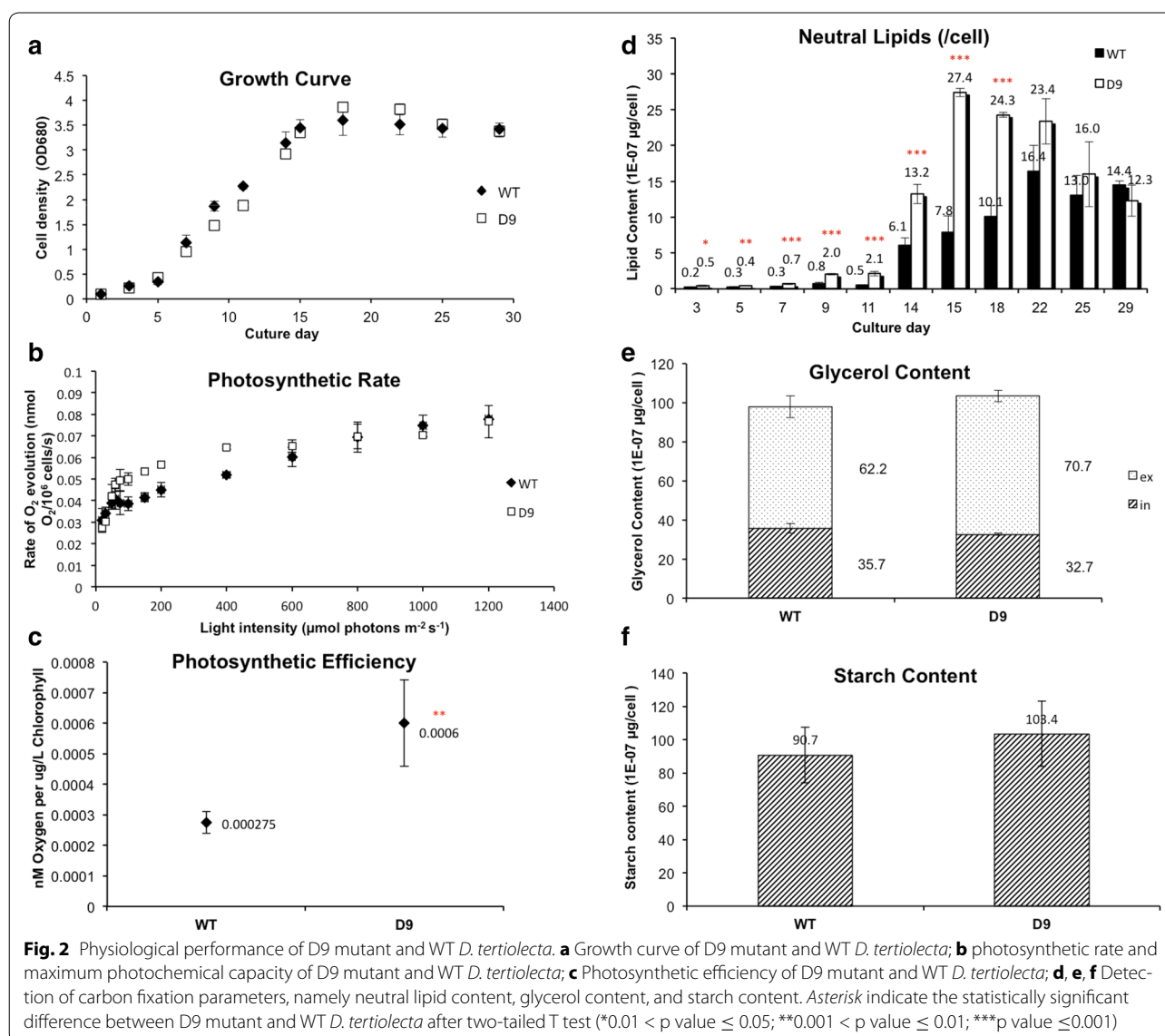
Functional annotation of the genes

Various strategies in optimizing growth conditions and phases have been suggested to stimulate production and accumulation of lipids or starch; these include expression of genes involved in lipids or starch biosynthesis and the maximization of the diversity of expressed genes [7, 9, 22–25]. To verify this and maximize the assembled outputs, sequencing results using different datasets for *de novo* assembly were compared: sequencing data from (1) wild-type only, (2) wild-type and D9 mutant and (3) enlarged Dt database with additional *D. tertiolecta* sample groups (Dt_v1, obtained from a wild-type *D. tertiolecta* strain cultured in a different growth phase, another random insertional mutant from *D. tertiolecta*) were then separately used to generate reference contigs and gene construction. From the comparison in Table 2, the enlarged Dt database Dt_v1 had more hit percentage and transcripts annotation, which was used for the following sections. The command line of BLASTX (from NCBI) was applied to the FASTA data generated from the *de novo* assembly, to obtain their functional assignments with reference to *C. reinhardtii* protein (Chlre4_best_proteins.fasta, Creinhardtii_169_peptide.fa, Creinhardtii_281_v5.5.protein.fa). By extracting the top hits with a BlastX E value $\leq 10^{-6}$, *D. tertiolecta* contigs were annotated. However, there were redundant *D. tertiolecta* contigs assembled with different lengths at distinct positions and junctions. To avoid redundant gene modeling, a filtering step was included with the E-value, confidence of assembled contigs and length of the contigs as the thresholds to select the top hit contig for the unique annotation name. The complete program used here was named as Bag2D-workflow (Blast1-annotation1-gene model1-Delete redundant genes-Blast2-annotation2-gene model2, namely protein name, transcriptID, geneID), using python language based scripts.

Although the contigs with E-value $\leq 10^{-6}$ may not be real transcripts, we decided to keep them to avoid complications with false negatives, accepting that the incidence of false positive could increase. In addition, different cutoff expectation values were set and compared afterwards.

Comparison of global transcriptome of D9 mutant with wild-type

The gene specific analysis generated from Partek Flow was imported into Partek Genomics Suite for statistical analyses. The data quality of log₂-transformed RPKM values for these two RNA-Seq datasets was checked using the sample histogram. The peak and trend of the curves indicated that the normalization method was suitable for this dataset and the RNA-Seq data were of



high quality and similarly distributed. Gene list was created with threshold of false discovery rate (FDR) ≤ 0.05 , multiple fold change (FC) ≥ 1.5 or ≤ -1.5 (to detect as many genes as possible that is different between the mutant and WT) and subsequently merged with the above generated annotation file with the common column of *D. tertiolecta* contig names (results were reported in Additional file 2). The annotated gene list created was used for further biological interpretation. Gene ontology (GO) enrichment categories also provided insights into differentially distributed protein functional families and categories. The up-regulated GOs were highly represented in the photosynthesis and ATP synthesis families, as shown in Fig. 4. Fatty acid synthesis requires stoichiometric amount of ATP, acetyl CoA and NADPH for each

two carbon added to the growing acyl chain [26]. Light-driven electron transport is coupled to ATP synthesis in chloroplasts [27]. Photosynthetic reactions are thus essential not only in providing a carbon source but also in generating reducing power (NADH and NADPH) and energy (ATP) for fatty acid synthesis [26]. According to this, mechanisms for enhanced lipid production could be elucidated, while comparable growth rate was observed between D9 mutant and WT cultures.

The KEGG pathway analysis showed that inositol phosphate metabolism, fatty acid biosynthesis, biosynthesis of secondary metabolites, fatty acid metabolism and purine metabolism were significantly correlated with higher lipid yield based on the cutoff of enrichment *p* value less than or equal to 0.05 (Additional file 3). From the

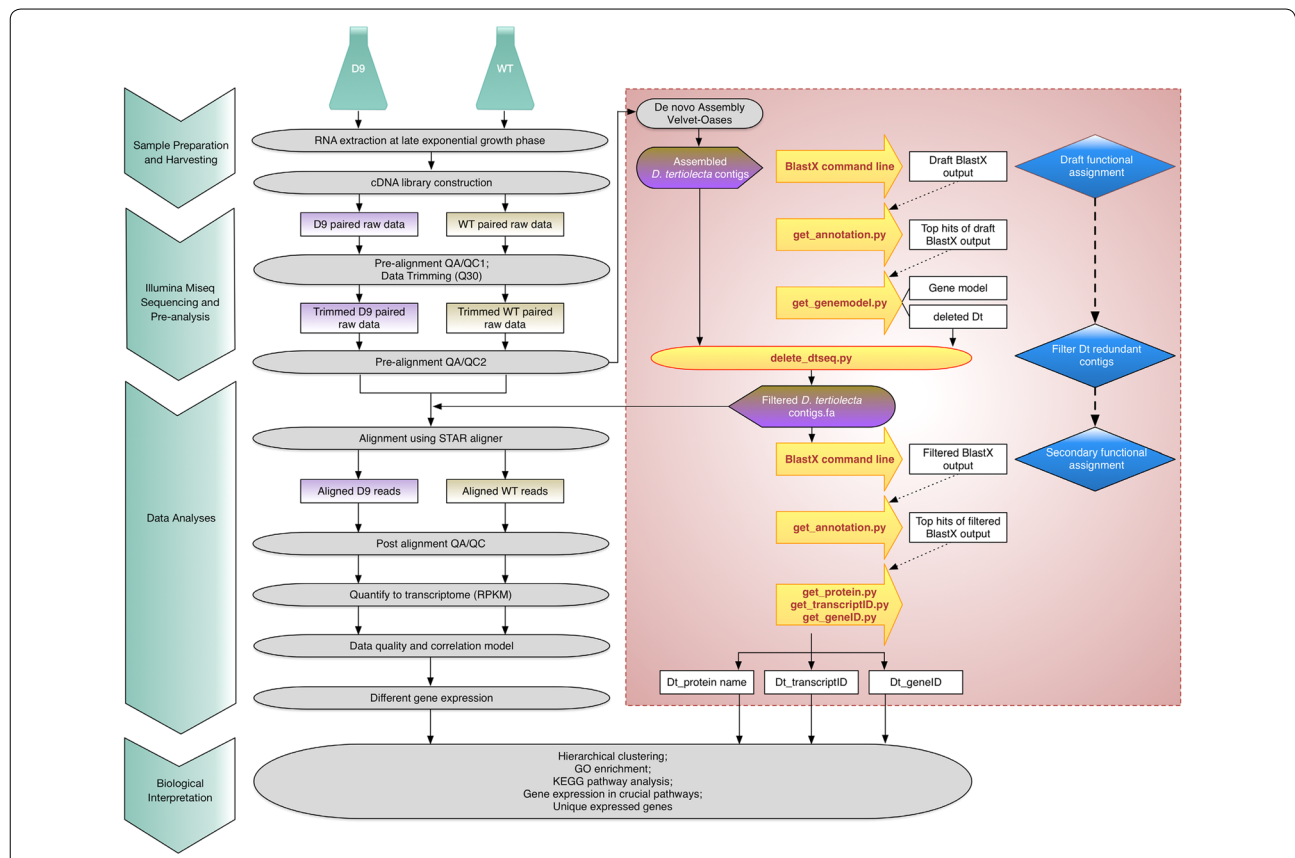


Fig. 3 RNA-Seq data analysis flowchart used in this study. The general pipeline includes sample preparation and harvesting, sequencing, data analyses, and biological interpretation. The red highlighted rectangle illustrates the construction of the *D. tertiolecta* reference library using Bag2D-workflow scripts. Bag2D: Blast1-annotation1-gene model1-Delete redundant genes-Blast2-annotation2-gene model2 (protein name, transcriptID, geneID)

Table 1 Run summary on the Illumina MiSeq platform

Sample name	Sequencing stats and pre-alignment QA/QC of raw data/pre-alignment QA/QC of post-trimming data					Post-alignment QA/QC after alignment	
	Total reads	Avg. read length	Avg. read quality	% N	% GC	Total reads	Aligned (%)
D9_S7_L001_R1	954,340/954,300	137.28/137.2	38/38.01	9.62E-04/0	47.74/47.73	954,300	56.72
D9_S7_L001_R2	954,340/954,300	137.07/136.98	37.69/37.7	1.04E-03/0	47.67/47.66		
WT_S8_L001_R1	1,084,599/1,084,546	136.67/136.59	38/38.01	1.11E-03/0	47.41/47.4	1,084,546	57.24
WT_S8_L001_R2	1,084,599/1,084,546	136.36/136.28	37.76/37.78	1.25E-03/0	47.34/47.33		

QA/QC Quality assurance and quality control

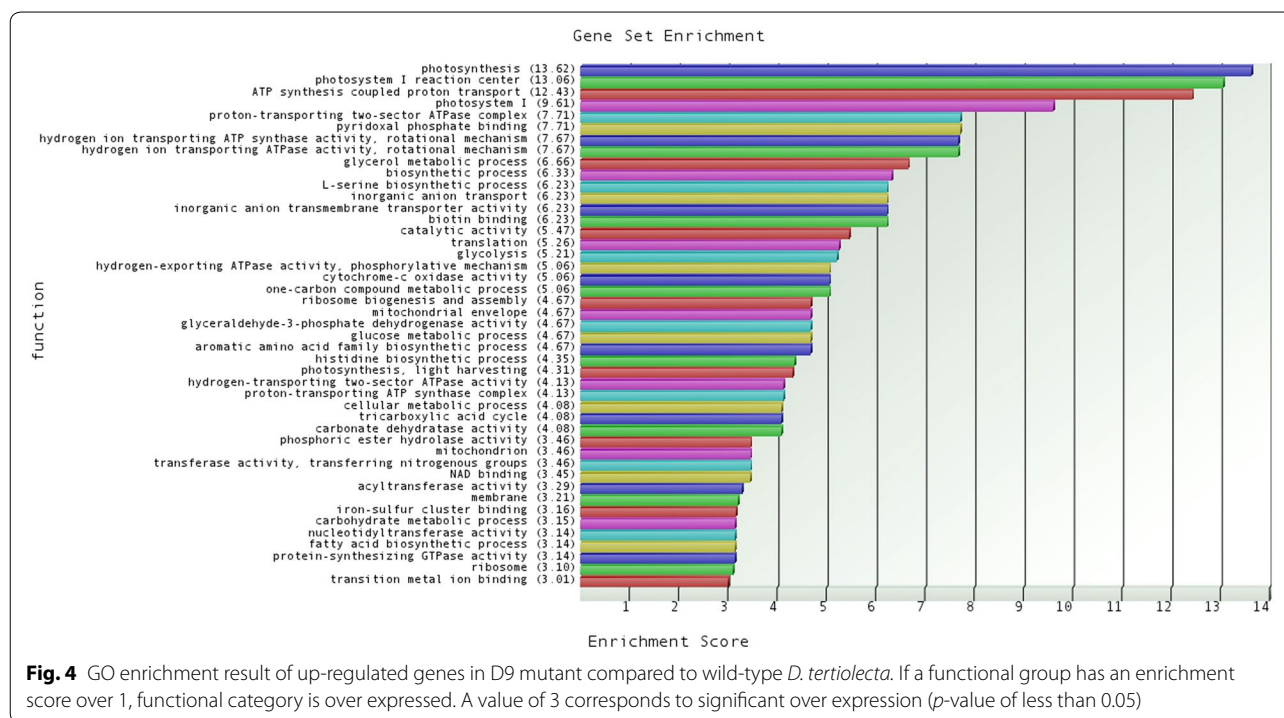
Avg. read quality >30 indicating 99.9% accuracy or greater

The ones in italic font were data generated from post-trimming

Table 2 Determining the reference transcripts through de novo assemblies using different sets of data

No.	Samples used for assembly	Size of the assembled file (MB)	Gene model	Number of non-redundant transcripts
(i)	WT	9.4	3818	14,903
(ii)	WT + D9	16.9	5360	23,564
(iii)	Enlarged Dt-1	45.8	7023	47,276

The BlastX cut-off value is E-value $\leq 10^{-6}$ for this comparison. The results of *D. tertiolecta* transcripts with BlastX hits to *C. reinhardtii* as reference



pathway analysis, the top two pathways with low-abundance contigs were the inositol phosphate metabolism and fatty acid biosynthesis pathways.

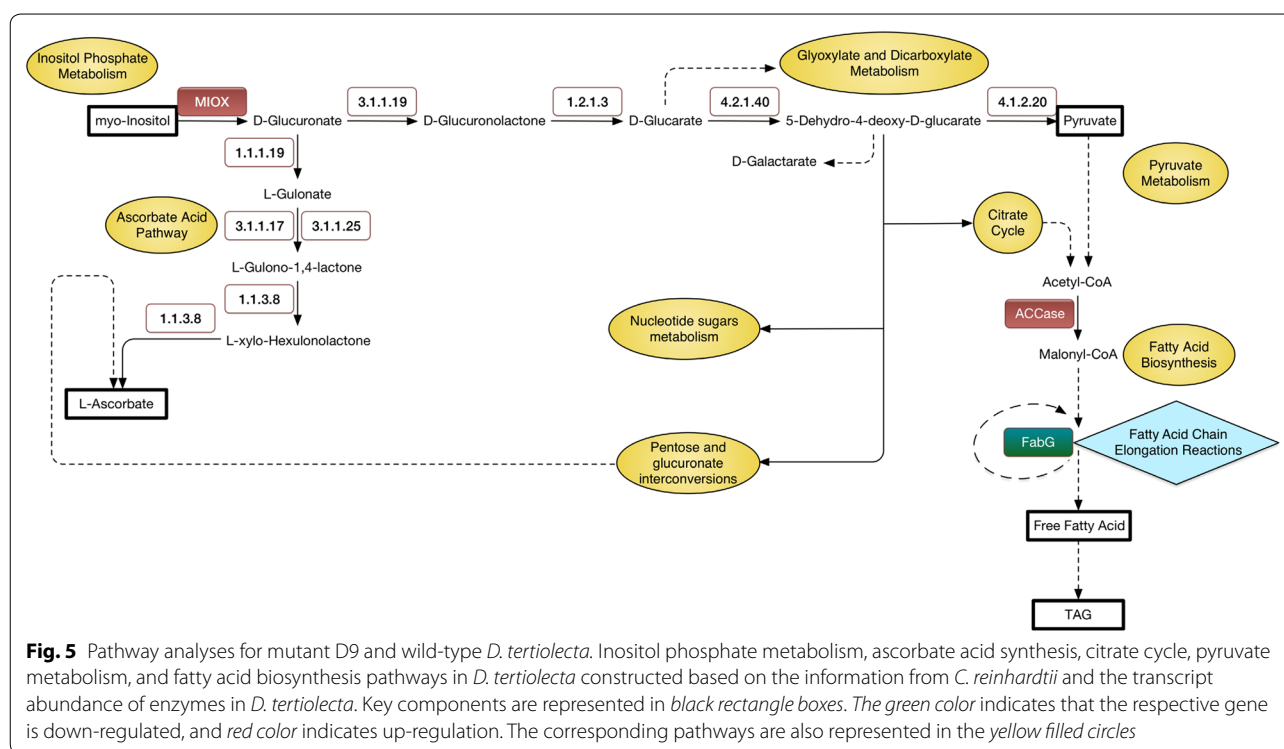
From the inositol phosphate metabolism, the gene that encodes myo-inositol oxygenase (MIOX) [EC: 1.13.99.1] showed significant up-regulation, which led to enhanced generation of D-Glucuronate as the substrate for both ascorbate acid synthesis pathway and generation of D-Glucarate. Fatty acid biosynthesis was the second top hit pathway. The up-regulated gene coding for ACCase [EC: 6.4.1.2] was detected in spite of a down-regulation of the gene (*FabG*) coding for 3-oxoacyl-[acyl-carrier protein] reductase [EC: 1.1.1.100], which is involved in the fatty acid chain elongation reactions.

In Fig. 5, we attempted to correlate the transcriptomic data with metabolite pathways. Changes within the metabolic intermediates with the metabolic pathways between D9 mutant and wild-type *D. tertiolecta*, namely the inositol phosphate metabolism, ascorbate acid synthesis, citrate cycle, pyruvate metabolism and fatty acid biosynthesis pathways were reconstructed based on the information from *C. reinhardtii* ChlamyCyc database [28] and the transcript abundance of enzymes in *D. tertiolecta*.

It is noted that the horizontal branch in the pathways in Fig. 5 goes into the production of pyruvate. No significant differentially expressed genes in glyoxylate and dicarboxylate metabolism were identified in D9 mutant as compared to WT.

Up-regulation of the gene coding for ACCase was observed. As ACCase catalyzes the first reaction of the fatty acid biosynthesis pathway, namely the formation of malonyl CoA from acetyl CoA and CO₂, its up-regulation may channel carbon flux to fatty acid synthesis. This suggests that concurrent over-expression of genes particularly in ACCase as the first committed step along the Inositol Phosphate Pathway and the Fatty Acid Biosynthesis Pathway will enhance neutral lipid production in algae.

To form a saturated fatty acid, the 3-ketoacyl ACP product is reduced by the enzyme FabG [29]. Herein, we predict that the down-regulation of the gene coding for FabG in the D9 mutant may change the length and saturation level of the fatty acid chain, leading to accumulation of more short-chain fatty acids or unsaturated fatty acids. The 16- or 18-carbon fatty acids are formed by a series of two-carbon chain elongating reactions catalyzed by a multi-subunit enzyme in most plants and algae [30]. Viscosity increases with fatty acid chain length [31] so that most plant TAGs have a viscosity range that is much higher than that of conventional diesel [32]. The higher viscosity results in poor fuel atomization in modern diesel engines, leading to problems derived from incomplete combustion such as carbon deposition and coking [33]. Medium-chain fatty acids (C8–C14) are favorable for production of biofuels, for they have properties that mimic current diesel fuels and they improve fluid characteristic of the liquid fuel [30, 34].



Pre-analysis for an additional D9 biological duplicate RNA-Seq data for validation was presented in Additional file 4. With more stringent criteria of $FC \geq 2$ or $FC \leq -2$ and $FDR \leq 0.05$, we found an overall similar pattern from gene expression profiles and KEGG pathway analysis results in Additional files 5 and 6. The expression levels of many genes in the metabolic pathways, photosynthesis pathways, carbon fixation pathways and fatty acid pathways were increased. Two randomly selected genes showed similar expression patterns in both real-time PCR and RNA-Seq (Additional file 7). This batch of experiment gave us a good hint that our results from the previous RNA-Seq experiment are reproducible.

Comparison of *D. tertiolecta* transcriptome database with other microalgae

Contigs from aforementioned Dt-1 database were compared to the transcripts/proteins from five other chlorophyta species with known genome sequences (*C. reinhardtii*, *C. subellipsoidea* C-169, *O. lucimarinus*, *V. carteri* and *C. variabilis* NC64A) by BlastN/BlastX. Compared with BlastX results, BlastN results retrieved fewer hits (Table 3). For example, 7023 *D. tertiolecta* contigs matched *C. reinhardtii* proteins using BlastX with a cut-off E-value of 10^{-6} indicating 35.97 % of the *C. reinhardtii* proteins could be assigned in *D. tertiolecta*, while only 611 (3.13 %) *D. tertiolecta* contigs matched *C. reinhardtii* using BlastN with cut-off E-value of 10^{-6} .

Similar patterns were also observed in the Blast results from the other three green algae at cut-off E-values of 0, 10^{-10} , 10^{-6} , 10^{-3} , respectively. This result indicates that the sequences of microalgae are more conserved at the protein level than that at the nucleotide level; therefore, BlastX results were subsequently used in this study for gene annotation.

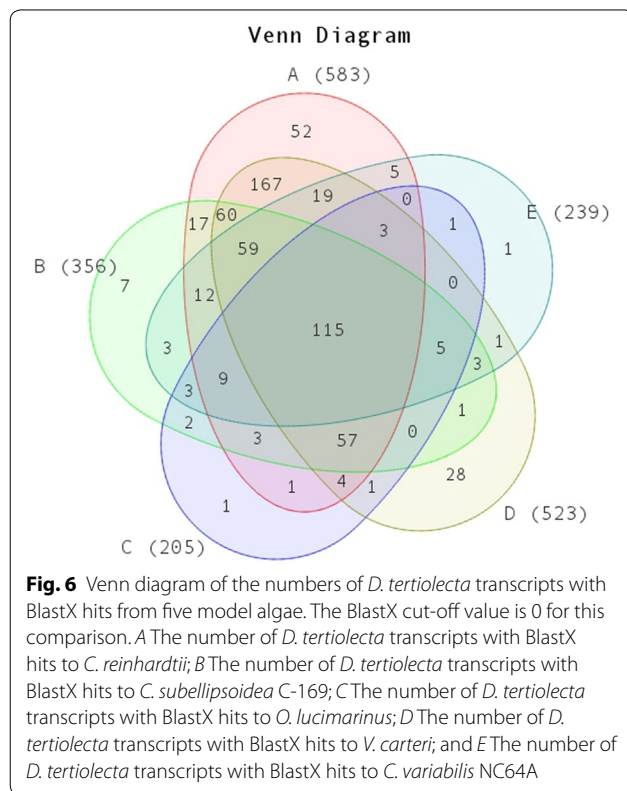
With the decrease of E-value stringency from 0 to 10^{-10} , 10^{-6} and 10^{-3} , the BlastX hit number for each transcript increased and the percentage of total contigs matching reference sequences increased (Table 3). To exclude possible false positives, only those contigs with E-value of 0 from BlastX results were used for identification of *D. tertiolecta* true genes. The results indicate that these six green algae have 115 contigs in common, and a total of 640 genes in *D. tertiolecta* could be annotated and identified (the overlaps and unique areas in the Venn diagram in Fig. 6) in the five references, while 583 contigs were in common with *C. reinhardtii*. From the Venn diagram in Fig. 6, some *Dunaliella* genes could not match that of the *Chlamydomonas* genes, but they do overlap with genes from the other four model algae. Through a comparison study on E-value from 0 to 0.1, the number of corresponding transcripts was plotted out in Fig. 7, and 10^{-6} was used as the threshold from the distribution of the hitting contigs. Therefore, a modification process was applied with a combination of identified *D. tertiolecta* transcripts from the BlastX results with the above

Table 3 Comparisons of homologues between *D. tertiolecta* and other five green algae with reference genome sequences

Algal reference	<i>Cre</i>	<i>Csu</i>	<i>Olu</i>	<i>Vca</i>	<i>ChIN</i>
Reference Transcripts or proteins #	19,526	9629	7796	15,285	9791
BlastN					
Transcript hit (E-value = 0)	82 (0.42 %)	18 (0.19 %)	0 (0.00 %)	24 (0.16 %)	20 (0.20 %)
Transcript hit (E-value $\leq 10^{-10}$)	574 (2.94 %)	229 (2.38 %)	15 (0.19 %)	246 (1.61 %)	281 (2.87 %)
Transcript hit (E-value $\leq 10^{-6}$)	611 (3.13 %)	249 (2.59 %)	16 (0.21 %)	269 (1.76 %)	307 (3.14 %)
Transcript hit (E-value $\leq 10^{-3}$)	654 (3.35 %)	252 (2.62 %)	16 (0.21 %)	278 (1.82 %)	315 (3.22 %)
BlastX					
Transcript hit (E-value = 0)	583 (2.99 %)	356 (3.70 %)	205 (2.63 %)	523 (3.42 %)	239 (2.44 %)
Transcript hit (E-value $\leq 10^{-10}$)	6610 (33.85 %)	5025 (52.19 %)	4002 (51.33 %)	6249 (40.88 %)	5106 (52.15 %)
Transcript hit (E-value $\leq 10^{-6}$)	7023 (35.97 %)	5643 (58.60 %)	4592 (58.90 %)	6986 (45.70 %)	5773 (58.96 %)
Transcript hit (E-value $\leq 10^{-3}$)	8561 (43.84 %)	6393 (66.39 %)	5267 (67.56 %)	8162 (53.40 %)	6604 (67.45 %)

The numbers before and within brackets are the number of *D. tertiolecta* transcripts with Blast hits from reference alga and the hitting percentage in the corresponding reference transcripts/proteins

Cre, *C. reinhardtii*; *Csu*, *C. subellipsoidea*; *Olu*, *O. lucimarinus*; *Vca*, *V. carteri*; *ChIN*, *C. variabilis* N64A



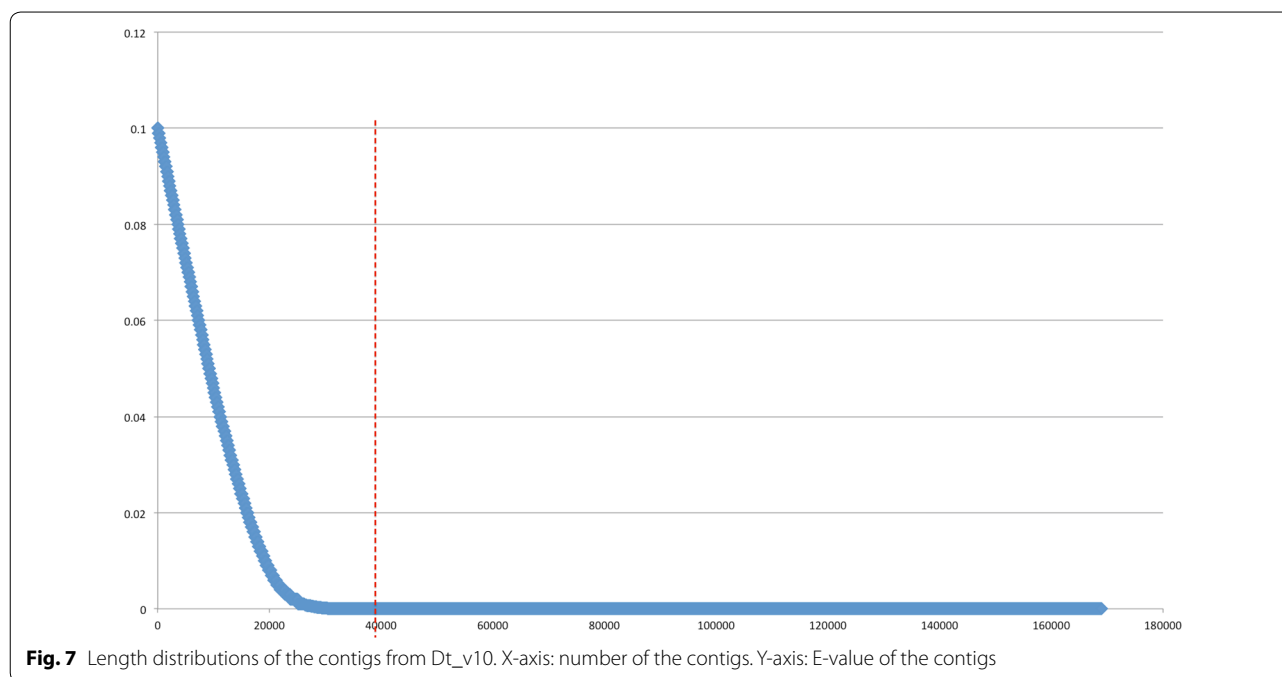
five green algae, by increasing E-value number to 10^{-6} BlastX for the construction of *D. tertiolecta* database.

Validation and optimization of the *D. tertiolecta* transcriptomic database

To validate the accuracy of the *D. tertiolecta* transcriptomic database from Bag2D, reported *D. tertiolecta*

nucleotides on National Center for Biotechnology Information (NCBI) were compared. The transcripts with the same *Chlamydomonas* protein annotation were compared in Table 4. The one with a higher lower E-value compared to the reference species will be used in the final *D. tertiolecta* database. From such comparison, we found that most contig sequences from Bag2D were identical compared to the NCBI published ones, as concluded from the high alignment scores generated from multiple alignment tools. Though we found some low alignment score pairs, which might caused by the existence of isoforms or errors of the online available sequences. Besides, we found there are some redundant nucleotides, like gi|46981381|gb|AY575952.1| *Dunaliella tertiolecta* assimilatory nitrate reductase (*nar*) gene (partial cds), gi|311818483|emb|HH768845.1| Sequence 5032 from Patent EP2221382, gi|18913154|gb|AY078279.1| *Dunaliella tertiolecta* assimilatory nitrate reductase (*nar*) mRNA (complete cds), with different NCBI ID numbers and names, which might cause misunderstanding. Some new genes have been found and the sequences are available, e.g., acetyl-coa carboxylase beta-carboxyltransferase subunit of plastidic multimeric ACCase, with the name of >Locus_2576_1Transcript_1/1_Confidence_1.000_Length_1955. The *D. tertiolecta* database was optimized with a better sequence or the original sequence elongated.

We optimized the *D. tertiolecta* transcriptome database mainly by two strategies: (1) Enlarging the *D. tertiolecta* transcriptome sequence in the database. Miseq output data after each run were included in the latest version and spiked with all the reported *D. tertiolecta* nucleotide sequences from NCBI to generate Dt_v10 after running through Bag2D pipeline and (2) annotating the *D.*



tertiolecta sequence with an addition of model high plant species. Considering the functional annotation of some microalgae may be problematic because annotation is largely based on plants and there is large phylogenetic distance between them. We also compared *D. tertiolecta* with a high-quality annotation of plant species *Arabidopsis thaliana*, using the latest large Dt merged database (Dt_v10). As a result, Dt_v10 database has a total 181 Mega-base nucleotides (481,381 contigs) ranging from 74 bps to 17,995 bps in length that were obtained for RNA-Seq alignment. The length distribution of the assembled transcripts was described in Fig. 8. Dt_v10-hit database (only including the contigs that can be annotated in Dt_v10 by 6 reference species) has a total 11 Mega-base nucleotides (10,185 contigs) with minimum length of 101 bps, maximum length of 15,975 bps and average length of 1106 bps (7052 was generated from *C. reinhardtii* and for RNA-Seq analysis). This allows us to identify a good quantity of *D. tertiolecta* gene sequences.

***Chlamydomonas* RNA-Seq data were used as the benchmark**

We used a set of *Chlamydomonas reinhardtii* RNA-Seq data as the benchmark to check the performance of Bag2D program and Partek software. Since *Chlamydomonas* has the genome sequence annotated, it can be performed in the standard way in the Partek Flow software for the alignment and annotation. It can also be assembled and annotated using in-house Bag2D software. From Additional file 8, we found 88 % of the

pathways were hit in both methods. A comparison of the top hit KEGG pathway generated from both methods was presented in Additional file 9, where a similar hit pattern of the over-representative genes in both methods were found.

Conclusions

This study provided a workflow (Bag2D) to construct a transcriptome database for the analysis of RNA-Seq data on the lipid-rich mutant. We have generated a lipid-rich microalgal mutant, named D9, via random mutagenesis. To characterize it on the transcriptomic level, RNA-Seq technology was applied and Bag2D was developed. After being validated in a model algal species *Chlamydomonas* as the benchmark, Bag2D is currently free for public access. It could serve as a model tool to construct transcriptome databases for those organisms without complete transcriptome information. Similarly, Hamid et al. [9] presented the first next-generation sequencing effort and transcriptome annotation of a non-model marine microalgae that is relevant to biofuel production by extracting cells from various growth conditions and different phases of growth cycle, using the 454 Genome Sequencer FLX with Titanium Chemistry. As a result, they identified 33,307 assembled isotigs, 409,789 unique isotigs and singletons and 8466 isotigs within E-value threshold of 10^{-6} . Despite their achievement, using Bag2D-workflow to analyze the RNA-Seq data from Illumina Miseq, we could obtain and identify more assembled contigs (181.2 MB) and unique transcripts (10,185

Table 4 Comparison studies of transcripts from Bag2D program and NCBI

<i>D. tertiolecta</i> transcripts from Bag2D	E-value	Length (bps)	<i>D. tertiolecta</i> nucleotide from NCBI	E-value	Length (bps)	Aligned score	Elongated
>Locus_1123_4Transcript_1/2_Confidence_0.800_Length_1500	0	1500	>gjl46981381 gjb AY575952.1 Dunaliella tertiolecta assimilatory nitrate reductase (nar) gene, partial cds	2e-18	1313	-	
			>gjl311818483 emb HH768845.1 Sequence 5032 from Patent EP2221382	0	2531	90.6	
			>gjl18913154 gjb AY078279.1 Dunaliella tertiolecta assimilatory nitrate reductase (nar) mRNA, complete cds	0	3447	90.6	+
>Locus_96_4Transcript_1/1_Confidence_1.000_Length_1881	0	1881	>gjl3869303 gjb AF065142.1 Dunaliella tertiolecta glutamine synthetase mRNA, partial cds	2e-109	601	92.8453	
>Locus_797_6Transcript_1/1_Confidence_1.000_Length_1463	1e-144	1463	>gjl2645974 gjb AF034201.1 Dunaliella tertiolecta proliferating cell nuclear antigen (PCNA) mRNA, partial cds	7e-122	616	97.8896	
>Locus_6018_7Transcript_2/2_Confidence_0.667_Length_959	2e-115	959	>gjl12232559 gjb AF036312.2 Dunaliella tertiolecta mitotic cyclin mRNA, partial cds	6e-47	490	96.1224	+
>Locus_1375_7Transcript_7/9_Confidence_0.632_Length_1220	1e-132	1220	>gjl167984 gjb M60049.1 DUNCAB D:tertiolecta 28.5-kDa LHClI apoprotein mRNA, complete cds	2e-132	1041	91.0663	
>Locus_169_2Transcript_3/5_Confidence_0.632_Length_1062	3e-122	1062	>gjl225322931 gjb F769282.1 Dunaliella tertiolecta ascorbate peroxidase mRNA, partial cds	1e-72	546	87.5458	
>Locus_1725_6Transcript_1/1_Confidence_1.000_Length_1811	0	1811	>gjl585087513 gjb KF193066.1 Dunaliella tertiolecta sedoheptulose-1,7-bisphosphatase (SBP) mRNA, complete cds	2e-180	1631	97.9767	
>Locus_613_6Transcript_1/1_Confidence_1.000_Length_1405	0	1405	>gjl682124627 gjb KJ930518.1 Dunaliella tertiolecta mitochondrial-activated protein kinase (MAPK) mRNA, complete cds	0	1687	90.3915	+
>Locus_284_4Transcript_1/1_Confidence_1.000_Length_1355	2e-16	1355	>gjl371532816 gjb JQ039042.1 Dunaliella tertiolecta ATP-dependent Clp protease proteolytic subunit (clpP) mRNA, complete cds; plastid	2e-16	1560	98.2288	
>Locus_17606_9Transcript_1/1_Confidence_1.000_Length_2042	0	2042	>gjl682124625 gjb KJ930517.1 Dunaliella tertiolecta phosphofructokinase (PFK) mRNA, complete cds	0	2049	99.3144	
>Locus_979_2Transcript_1/2_Confidence_0.833_Length_2662	4e-139	2662	>gjl144601644 gjb EF471039.1 Dunaliella tertiolecta isolate 1 NRT2 (Nrt2) gene, partial cds	5e-50	644	94.4099	
>Locus_1062_4Transcript_1/1_Confidence_1.000_Length_630	2e-82	630	>gjl19879329 gjb AY032598.1 Dunaliella tertiolecta nucleoside diphosphate kinase mRNA, complete cds	7e-57	840	42.5397	*
>Locus_2576_1Transcript_1/1_Confidence_1.000_Length_1955	0	1955	>gjl459938225 gjb KC572136.1 UNVERIFIED:Dunaliella tertiolecta isolate PL1 acetyl-CoA carboxylase beta subunit-like (accD) gene, partial sequence; chloroplast	1e-42	925	44.973	
>Locus_468_7Transcript_1/1_Confidence_1.000_Length_1448	0	1448	>gjl1165328 gjb AF038570.1 Dunaliella tertiolecta cyclin-dependent kinase 1 (DUNCDC2) mRNA, complete cds	0	1061	99.7172	
>Locus_652_4Transcript_1/1_Confidence_1.000_Length_2435	0	2435	>gjl371532796 gjb JQ039032.1 Dunaliella tertiolecta ATP synthase CF1 alpha subunit (atpA) mRNA, complete cds; plastid	0	1515	42.8383	*

Table 4 continued

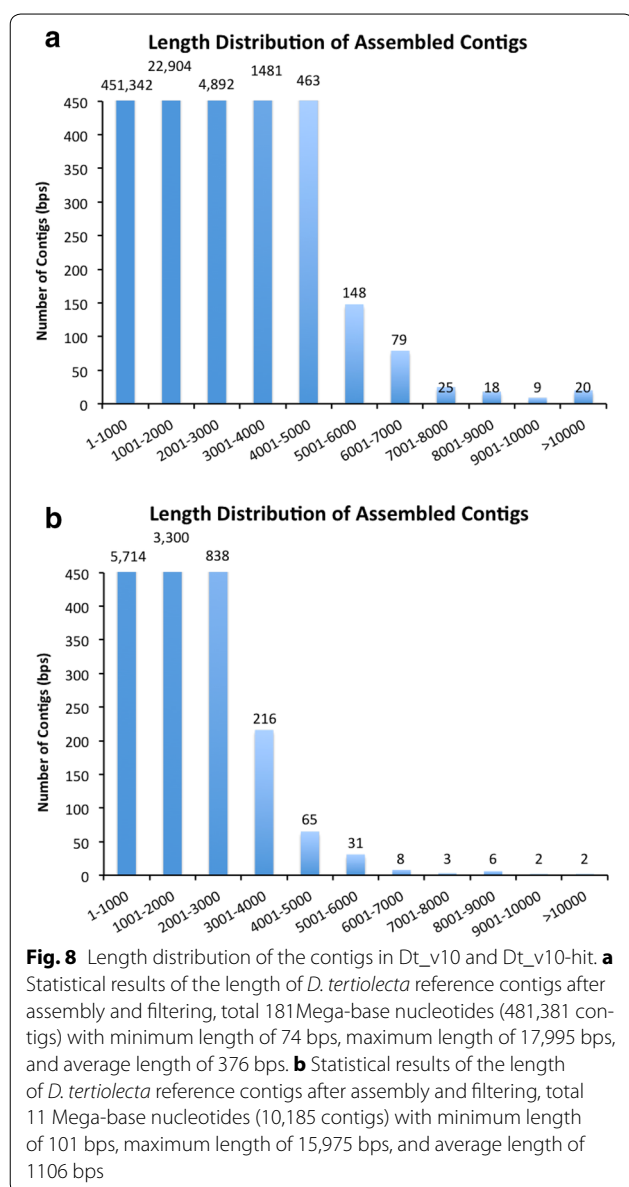
<i>D. tertiolecta</i> transcripts from Bag2D	E-value	Length (bps)	<i>D. tertiolecta</i> nucleotide from NCBI	E-value	Length (bps)	Aligned score	Elongated
>Locus_7608_9Transcript_1/1_Confidence_1.000_ Length_2170	0	2170	>gij371532798 gb JQ039033.1 Dunaliella tertiolecta ATP synthase CF1 beta subunit (atpB) mRNA, partial cds; plastid	5e-177	1167	46.8723	*
>Locus_3958_1Transcript_1/1_Confidence_1.000_ Length_2042	0	2042	>gij371532912 gb JQ039091.1 Dunaliella tertiolecta elongation factor Tu (tufA) mRNA, complete cds; plastid	8e-154	1257	47.494	
>Locus_3579_4Transcript_1/1_Confidence_1.000_ Length_943	1e-64	943	>gij371532800 gb JQ039034.1 Dunaliella tertiolecta ATP synthase CF1 epsilon subunit (atpE) mRNA, complete cds; plastid	3e-07	408	26.4706	*
>Locus_6870_1Transcript_3/3_Confidence_0.778_ Length_1870	1e-117	1870	>gij761262915 gb KJ9530371.1 Dunaliella tertiolecta glu- cose-6-phosphate dehydrogenase (G6PDH) mRNA, complete cds; chloroplast	3e-72	3246	34.6524	*

BlastX with *C. reinhardtii* using cut-off value at E-value $\leq 10^{-6}$ for this comparison

The one in italic font was chosen in the database optimization for each gene

+, the NCBI nucleotide was chosen for the corresponding gene, but it was elongated by part of the sequence from Bag2D

*, the two nucleotides did not quite match from the two methods, which may have been caused by the existence of isoforms or errors of the one from NCBI (determined by E-value and analyses of the sequences)



transcripts, with E-value threshold of 10^{-6}) with functional assigned.

From the RNA-Seq result, it can be seen that elimination of the gene (*FabG*) coding for 3-oxoacyl-[acyl-carrier protein] reductase can relieve the feedback inhibition of β -ketoacyl-ACP synthase (*fabB* or *fabH*) caused by the accumulation of fatty acyl-ACPs [35] and terminate the chain elongation cycle [19], along with the boosting of rate-limiting precursor (malonyl-CoA) flux by the expression of the acetyl-CoA carboxylase (ACCase), which leads to the D9 mutant producing about 2- to 4-fold more fatty acids. The upstream enzyme myo-inositol oxygenase was overexpressed to convert more precursors for the biosynthesis

of fatty acid. In addition, from KEGG pathway analysis and GO enrichment analysis, many photosynthesis-related genes were found to be overexpressed. Photosynthetic rate measurement also proved that more energy was generated from photosynthesis in the mutant. Based on the results, it appears that this workflow is able to provide biological insights into the expression patterns of transcripts associated with energy metabolism and carbon flow pathways. This multiple pathway engineering approach that focuses on optimizing the expression of several related pathways is potentially useful for gene manipulation that can be directly applied to engineering microalgal fatty acid production.

Methods

Culture strains and culture condition

Dunaliella tertiolecta strain UTEX LB-999 was obtained from the UTEX Culture Collection of Algae (University of Texas at Austin, TX, USA). *D. tertiolecta* cells were grown in flasks in sterile ATCC-1174 DA liquid medium (American Type Culture Collection at Manassas, Virginia) containing 0.5 M NaCl incubated on a rotary shaker at 25 °C, under 12 h light/12 h dark with light intensity of 30 $\mu\text{mol photons m}^{-2} \text{s}^{-1}$. For the purpose of clarity, work conducted throughout the paper is based on biological and technical triplicates unless otherwise stated.

Dunaliella tertiolecta transformation and mutant screening

The pGreenII0000 plasmid incorporated a 431-bps *CrRBCS2* promoter and a 526-bps bleomycin resistance gene (*ble*) to confer zeocin-resistance [36] was designed and constructed in our laboratory.

D. tertiolecta cells were transformed using the glass bead method [37] with minor modifications. Cultures grown for 5 days in sterile ATCC-1174 DA liquid medium containing 0.08 M NaCl were harvested by centrifugation ($3000\times g$, 10 min) and resuspended in 0.08 M NaCl ATCC-1174 DA liquid medium to a cell concentration of $1-2 \times 10^8 \text{ cell mL}^{-1}$. A 300- μl aliquot of this cell suspension was added to a 12-mL round-bottom tube containing 0.3 g acid-washed glass beads (425–600 μm diameter; Sigma), 100 μl 20 % polyethylene glycol (PEG-8000; Sigma), 1 μg linearized plasmid and 5 μl fish sperm DNA. After vortexing for 20 s at maximum speed, the cells were plated immediately onto 0.08 M NaCl ATCC-1174 DA medium agar plates containing 10 $\mu\text{g mL}^{-1}$ zeocin (Invitrogen). Colonies that appeared within 3 weeks were picked and inoculated into 0.5 M NaCl ATCC liquid medium. Secondary selection in 0.08 M NaCl ATCC medium with 5 $\mu\text{g mL}^{-1}$ zeocin was performed to reduce the false-positive transformants.

Determination of cell growth and quantitative lipid measurement

Cell concentration was counted twice a day to monitor the growth of the culture. Stationary phase was reached when the cell concentration and optical density (OD₆₈₀) remained constant. The growth kinetic study was repeated at least three times.

Fatty acid methyl esters (FAMES) were prepared by direct transmethylation with sulfuric acid in methanol [38]. The FAMES were analyzed by gas chromatograph (model 7890B, Agilent Technologies) equipped with a mass-selective detector (model 5977A, Agilent Technologies) [39, 40].

Nile red staining quantification method offers an indirect measurement for lipids, binding specifically to neutral lipids, which is the most commonly used lipophilic stain for intracellular TAG detection in microalgae [41]. Nile Red measurement was found to parallel that of the GC measurement, and since Nile Red method is a rapid, we mainly measured lipid by Nile Red and report here using Chen's protocol [42] with minor modification. Cells were collected every 2 days from mutants and wild-type *D. tertiolecta*. Cell concentration was estimated using OD₆₈₀. Cells were harvested by centrifugation at 3000×g for 10 min and resuspended in fresh ATCC-1174 DA liquid medium with the same salinity, to an OD₆₈₀ of 0.3. Two hundred microliters of cell samples, culture medium blank and triolein standard were transferred to a 96-well black, clear-bottom plate. The plate was read at the excitation and emission wavelength at 524 nm and 586 nm, respectively, before and after addition of 2 μl Nile red working solution prepared in acetone [42] and incubated for 5 min in the dark.

Determination of photosynthetic rate and photosynthetic efficiency

The mutants and wild-type *D. tertiolecta* cells were collected on day 15 by centrifugation at 12,000×g for 15 min at 4 °C. The high centrifugal force served to weaken the cell structures to facilitate extraction of chlorophyll. Chlorophyll content of individual sample was estimated spectrophotometrically [43]. Subsequently, photosynthetic performance was carried out using an oxygen electrode according to the operating manual (Rank Brothers, Bottisham, Cambridge, UK).

Determination of glycerol and starch content

One milliliter of the D9 and wild-type *D. tertiolecta* liquid culture at stationary phase (day 15) was harvested for the determination of intra- and extracellular glycerol contents. The level of glycerol was determined using Free Glycerol Determination Kit (Sigma FG0100), according to the protocol provided by the manufacturer. Ten

milliliters of the *D. tertiolecta* cells at stationary phase was collected and the starch content was determined using Starch Assay kit (Sigma STA20), according to the instructions provided by the manufacturer.

Construction of cDNA libraries for next-generation sequencing analysis

Total RNA of D9, WT was extracted on day 8 from *D. tertiolecta* cells using an RNeasy[®] Plant Mini Kit (Qiagen, Valencia, CA, USA), according to manufacturer's protocol. Approximately 2 μg of the resulting total RNA was used for synthesis of cDNA using the TruSeq Stranded Total RNA LT Sample Prep Kit (with Ribo-Zero Plant) (Illumina) according to manufacturer's instruction including synthesis of first and second strands cDNA, end repair, 3'-end adenylaton, adapter ligation, fragment enrichment (e.g., ~350 bps, in length), library validation and quantification. The libraries were sequenced using Illumina MiSeq Sequencer (Illumina, Inc., San Diego, CA, USA) according to the manufacturer's instructions. To check the variance from the effect of RNA-Seq technology on the mutant and wild-type samples, we extracted another set of duplicate samples on Day 12, and the same process was carried out as the previous experiment group.

De novo assembly of Illumina short reads and RNA-Seq data processing

The FASTQ datasets of *D. tertiolecta* generated from Illumina MiSeq were imported into Partek[®] Flow[®] software (version 3.0 Copyright©; 2014 Partek Inc., St. Louis, MO, USA) for quality assessment. The raw data were then trimmed from both ends based on the following parameter setting: min read length = 25; quality encoding = auto detect; end min quality level (Phred) = 20. *D. tertiolecta* database was *de novo* assembled via Velvet and subsequently Oases assembler. The parameters used for Velvet assembly were as follows: hash length = 21; expected coverage = 10; max coverage = 500; min coverage = 1; min contig length = 50; min long cutoff = 2; max branch length = 100; max divergence rate = 0.2; max gap count = 3; min read-pair validation = 10. The parameters used for Oases assembly were as follows: coverage cutoff = 3; min paired cutoff = 4; min observed to estimate ratio = 0.01; edge sensitivity = 0.01; contig uniqueness = 3. A user-friendly script count_geneLength.py was used to determine the length of the assembled contigs.

The paired-end reads were mapped back to the assembled contigs. Data aligned to the transcriptome in RNA-Seq analysis were selected to estimate transcript abundance. Gene-specific analysis was subsequently used to compare the samples from mutant D9 and WT at transcript level using the default setting (Poisson model was used). Read hits per contig were normalized to RPKM

(Reads Per Kilobase per Million mapped reads) used for estimation at transcription level. One-way ANOVA analysis was used for the differentially expressed transcripts in at least one comparison for day 12 RNA-Seq data.

Comparisons among other green algae and high plant species

The FASTA files of transcripts and proteins sequence of *C. reinhardtii*, *V. carteri*, *C. subellipsoidea* C-169, *C. variabilis* NC64A were downloaded from JGI website (<http://www.jgi.doe.gov>) and *Arabidopsis thaliana* from the Arabidopsis Information Resource (<http://www.arabidopsis.org>) and used as reference sequences for alignment with *D. tertiolecta* transcripts as query sequences. The *D. tertiolecta* hit profiles among different species were compared.

Optimization of the *D. tertiolecta* database and Bag2D program

To make the *D. tertiolecta* database more complete and accurate, more Miseq RNA-Seq data were included together with the NCBI published sequence information. Since the Bag2D program is in-house constructed, we validate it using a set of RNA-Seq data from *Chlamydomonas* as a benchmark.

Functional annotation of the *D. tertiolecta* contigs and biological interpretation

D. tertiolecta is a species that has not been sequenced or annotated. Using the reference genome of related species such as *C. reinhardtii* or *V. carteri* or *C. subellipsoidea* C-169, and *C. variabilis* NC64A, the percentages of hit for *D. tertiolecta* in Partek Flow STAR aligner were less than 5 % (data not shown). To improve the hits, a novel Bag2D-workflow program using python language based scripts was developed. A typical run of Bag2D consists of two steps. From the precursor *de novo* assembly that was obtained from the Partek Flow using Velvet + Oases, a set of blast output was generated by BlastX using the query information of *D. tertiolecta* transcript list and the reference protein sequences of related species with a customer e value of E-value $\leq 10^{-6}$. Subsequently, *D. tertiolecta* contigs were selected from the top hits, and genes with reference to the model organisms were constructed. The redundant transcripts were filtered using a “delete” program. With the remaining *D. tertiolecta* contigs, BlastX was conducted for a second time. The corresponding gene ID, transcript ID and protein name were sorted and the resulting files were used as a new ‘annotation’ file (on the author’s Github page) to perform further gene analysis and biological interpretation by Partek® Genomics Suite® software (version 6.6 Copyright©; 2014 Partek Inc., St. Louis, MO, USA). The two steps were carried out by the

user-friendly scripts `extract_blast.py`, and `get_geneID/transcriptID/proteinname.py` (including `count_geneLength.py`). The steps of the Bag2D-workflow appear as red box in Fig. 3. The gene-specific analysis was subsequently imported into PGS with the annotation file. They were merged according to the name of *D. tertiolecta* contigs. The annotated data were used to perform GO enrichment with a modified *C. reinhardtii* GO annotation file downloaded from JGI website (<http://www.jgi.doe.gov>), using Fisher’s Exact test with a restrict analysis of more than two genes. The representative pathways were generated using pathway analysis tool, by Fisher’s Exact test and the *C. reinhardtii* KEGG database (<http://www.genome.jp/>). The novel Bag2D program package and computationally processed *Dunaliella tertiolecta* draft transcriptome database and its annotation files are hosted at the author’s GitHub page <https://github.com/SPURc-Lab/NGS-D9> with the step-by-step user manual for public access. The raw data from RNA-Seq and processed files were deposited into GEO with accession number of GSE70876. We have made the simulation data for this experiment available on the website.

Additional files

Additional file 1. Linear regression of Nile red assay and GC–MS measurement. Horizontal error bars show standard deviation for Nile red assay; Vertical error bars show standard deviation for GC–MS assay. The line shows linear regression between the two methods. Strain genotypes 1, 3, and 5 represent culture days 8, 13, and 16 for wild-type strain, respectively; 2, 4, and 6, represent culture days 8, 13, and 16 for D9 mutant strain. All experiments were performed in triplicate.

Additional file 2. D9 and wild-type *Dunaliella tertiolecta* RNA-Seq result.

Additional file 3. D9 and wild-type *Dunaliella tertiolecta* KEGG pathway analysis results of RNA-Seq first run. The top hit pathways in pathway analysis with p value ≤ 0.05 .

Additional file 4. Run summary of second round of D9 duplicate samples on the Illumina MiSeq platform.

Additional file 5. D9 and wild-type *Dunaliella tertiolecta* One-way ANOVA results of RNA-Seq second run.

Additional file 6. D9 and wild-type *Dunaliella tertiolecta* KEGG pathway analysis results of RNA-Seq second run. The top hit pathways in pathway analysis with p value ≤ 0.05 .

Additional file 7. Comparison of gene expression profiles from real-time PCR and RNA-Seq. a) The ratio of Locus_1462_2Transcript_1/2 expression level in D9 compared to wild-type *D. tertiolecta* is 7.8 from qPCR and 9.6 from RNA-Seq. b) The ratio of Locus_15808_1Transcript_1/1 expression level in D9 compared to wild-type *D. tertiolecta* is 6.2E – 04 from qPCR and 1.1E – 06 from RNA-Seq.

Additional file 8. Comparison of two different methods to analyze *Chlamydomonas* RNA-Seq data. ✓ - The identical pathways in the two methods.

Additional file 9. Comparison of the top hit pathway—Oxidative Phosphorylation Pathway from the two methods. a) Using *Chlamydomonas* genome information to do the alignment and annotation to analyze the RNA-Seq data. b) Using the Bag2D program to construct the *Chlamydomonas* database, and use the self-constructed Cre database for the RNA-Seq data analyses.

Abbreviations

NGS: next-generation sequencing; Bag2D-workflow: Blast1-annotation1-gene model1-Delete redundant genes-Blast2-annotation2-gene model2; TAGs: triacylglycerols; ACCase: acetyl-CoA carboxylase; DGAT: diacylglycerol acyltransferase; PDAT: phospholipid: diacylglycerol acyltransferase; ME: malic enzyme; FAS: fatty acid synthase; PEPC: phosphoenolpyruvate carboxylase; FDR: false discovery rate; FC: multiple fold change; GO: gene ontology; KEGG: Kyoto encyclopedia of genes and genomes; MIOX: myo-inositol oxygenase; FabG: 3-oxoacyl-[acyl-carrier protein] reductase; *ble*: bleomycin resistance gene.

Authors' contributions

LY carried out the physiological studies, molecular engineering and NGS work. TWT guided in NGS data analyses and code optimization. YKN helped in cDNA library preparation and revised the manuscript. KHB reviewed the code, participated in designing the validation experiment, and revised the manuscript. HS participated in experiment design, coordination, and in revising the manuscript. HL provided the original backbone plasmid, participated in the modification of the neutral lipid quantification method, and revised the manuscript. LY, YKL and TWT analyzed the data and drafted the manuscript. All authors read and approved the final manuscript.

Author details

¹ Department of Microbiology and Immunology, Yong Loo Lin School of Medicine, National University of Singapore, Singapore, Singapore. ² Department of Biochemistry, Yong Loo Lin School of Medicine, National University of Singapore, Singapore, Singapore. ³ Institute of Molecular and Cell Biology, A*STAR, Singapore, Singapore.

Acknowledgements

This work was funded by the National Research Foundation (NRF), Prime Minister's Office, Singapore, under its Campus for Research Excellence and Technological Enterprise (CREATE) Programme (Grant No. R-182-000-205-592). The authors wish to acknowledge Mr Chin-Seng Low from Department of Microbiology and Immunology, Yong Loo Lin School of Medicine, National University of Singapore for the general lab supply, Mr Yuan Yao from College of Computer Science and Technology, Zhejiang University for the python language guidance in the construction of the NGS platform, Mr Erwin Tantoso and Ms Hsiufen Chua from Partek SG Pte. Ltd. for the instructions in using Partek software suite.

Competing interests

The authors declare that they have no competing interests.

Received: 30 March 2015 Accepted: 13 November 2015

Published online: 25 November 2015

References

- US Energy Information Administration [database on the Internet]. Available from: <http://www.eia.gov> (US Energy Information Administration, 2014).
- Hu Q, Sommerfeld M, Jarvis E, Ghirardi M, Posewitz M, Seibert M, et al. Microalgal triacylglycerols as feedstocks for biofuel production: perspectives and advances. *Plant J*. 2008;54(4):621–39.
- Widjaja A, Chien C-C, Ju Y-H. Study of increasing lipid production from fresh water microalgae *Chlorella vulgaris*. *J Taiwan Inst Chem E*. 2009;40(1):13–20.
- Dellomonaco C, Fava F, Gonzalez R. The path to next generation biofuels: successes and challenges in the era of synthetic biology. *Microb Cell Fact*. 2010;9(3):1–15.
- Barzegari A, Hejazi MA, Hosseinzadeh N, Eslami S, Aghdam EM, Hejazi MS. *Dunaliella* as an attractive candidate for molecular farming. *Mol Biol Rep*. 2010;37(7):3427–30.
- Ben-Amotz A, Polle JE, Rao DS. The alga *Dunaliella*: biodiversity, physiology, genomics and biotechnology. NH: Science Publishers Enfield; 2009.
- Goyal A. Osmoregulation in *Dunaliella*, Part II: photosynthesis and starch contribute carbon for glycerol synthesis during a salt stress in *Dunaliella tertiolecta*. *Plant Physiol Bioch*. 2007;45(9):705–10.
- Hosseini Tafreshi A, Shariati M. *Dunaliella* biotechnology: methods and applications. *J Appl Microbiol*. 2009;107(1):14–35.
- Rismani-Yazdi H, Haznedaroglu BZ, Bibby K, Peccia J. Transcriptome sequencing and annotation of the microalgae *Dunaliella tertiolecta*: pathway description and gene discovery for production of next-generation biofuels. *BMC Genom*. 2011;12(1):148.
- Takagi M, Yoshida T. Effect of salt concentration on intracellular accumulation of lipids and triacylglyceride in marine microalgae *Dunaliella* cells. *J Biosci Bioeng*. 2006;101(3):223–6.
- Courchesne NMD, Parisien A, Wang B, Lan CQ. Enhancement of lipid production using biochemical, genetic and transcription factor engineering approaches. *J Biotechnol*. 2009;141(1):31–41.
- Blanc G, Agarkova I, Grimwood J, Kuo A, Brueggeman A, Dunigan DD, et al. The genome of the polar eukaryotic microalga *Coccomyxa subellipsoidea* reveals traits of cold adaptation. *Genome Biol*. 2012;13(5):R39.
- Blanc G, Duncan G, Agarkova I, Borodovsky M, Gurnon J, Kuo A, et al. The *Chlorella variabilis* NC64A genome reveals adaptation to photosymbiosis, coevolution with viruses, and cryptic sex. *Plant Cell*. 2010;22(9):2943–55.
- Merchant SS, Prochnik SE, Vallon O, Harris EH, Karpowicz SJ, Witman GB, et al. The *Chlamydomonas* genome reveals the evolution of key animal and plant functions. *Science*. 2007;318(5848):245–50.
- Palenik B, Grimwood J, Aerts A, Rouz  P, Salamov A, Putnam N, et al. The tiny eukaryote *Ostreococcus* provides genomic insights into the paradox of plankton speciation. *Proc Natl Acad Sci USA*. 2007;104(18):7705–10.
- Prochnik SE, Umen J, Nedelcu AM, Hallmann A, Miller SM, Nishii I, et al. Genomic analysis of organismal complexity in the multicellular green alga *Volvox carteri*. *Science*. 2010;329(5988):223–6.
- Radakovits R, Jinkerson RE, Fuerstenberg SI, Tae H, Settlage RE, Boore JL, et al. Draft genome sequence and genetic transformation of the oleaginous alga *Nannochloropsis gaditana*. *Nature Commun*. 2012;3:686.
- Yang S, Guarneri MT, Smolinski S, Ghirardi M, Pienkos PT. De novo transcriptomic analysis of hydrogen production in the green alga *Chlamydomonas moewusii* through RNA-Seq. *Biotechnol Biofuels*. 2013;6(1):118.
- Xu P, Gu Q, Wang W, Wong L, Bower AG, Collins CH, et al. Modular optimization of multi-gene pathways for fatty acids production in *E. coli*. *Nature Commun*. 2013;4:1409.
- Radakovits R, Jinkerson RE, Darzins A, Posewitz MC. Genetic engineering of algae for enhanced biofuel production. *Eukaryot Cell*. 2010;9(4):486–501.
- Gee R, Goyal A, Byerrum RU, Tolbert NE. Two isoforms of dihydroxyacetone phosphate reductase from the chloroplasts of *Dunaliella tertiolecta*. *Plant Physiol*. 1993;103(1):243–9.
- Hirokawa T, Hata M, Takeda H. Correlation between the starch level and the rate of starch synthesis during the developmental cycle of *Chlorella ellipsoidea*. *Plant Cell Physiol*. 1982;23(5):813–20.
- Ratledge C. Fatty acid biosynthesis in microorganisms being used for single cell oil production. *Biochimie*. 2004;86(11):807–15.
- Ramazanov A, Ramazanov Z. Isolation and characterization of a starchless mutant of *Chlorella pyrenoidosa* STL-PI with a high growth rate, and high protein and polyunsaturated fatty acid content. *Phycol Res*. 2006;54(4):255–9.
- Wang ZT, Ullrich N, Joo S, Waffenschmidt S, Goodenough U. Algal lipid bodies: stress induction, purification, and biochemical characterization in wild-type and starchless *Chlamydomonas reinhardtii*. *Eukaryot Cell*. 2009;8(12):1856–68.
- Li-Beisson Y, Shorrosh B, Beisson F, Andersson MX, Arondel V, Bates PD et al. Acyl-lipid metabolism. The *Arabidopsis* book/American Society of Plant Biologists. 2013;11.
- Allen JF. Photosynthesis of ATP-electrons, proton pumps, rotors, and poise. *Cell*. 2002;110(3):273–6.
- May P, Christian J-O, Kempa S, Walther D. ChlamyCyc: an integrative systems biology database and web-portal for *Chlamydomonas reinhardtii*. *BMC Genom*. 2009;10(1):209.
- Sharma SK, Kapoor M, Ramya T, Kumar S, Kumar G, Modak R, et al. Identification, characterization, and inhibition of *Plasmodium falciparum* β -hydroxyacyl-acyl carrier protein dehydratase (*FabZ*). *J Biol Chem*. 2003;278(46):45661–71.
- Durrett TP, Benning C, Ohlrogge J. Plant triacylglycerols as feedstocks for the production of biofuels. *Plant J*. 2008;54(4):593–607.

31. Chow CK. Fatty acids in foods and their health implications. CRC Press; 2007.
32. Knothe G, Steidley KR. Kinematic viscosity of biodiesel fuel components and related compounds. Influence of compound structure and comparison to petrodiesel fuel components. *Fuel*. 2005;84(9):1059–65.
33. Ryan T III, Dodge L, Callahan T. The effects of vegetable oil properties on injection and combustion in two different diesel engines. *J Am Oil Chem Soc*. 1984;61(10):1610–9.
34. Blatti JL, Beld J, Behnke CA, Mendez M, Mayfield SP, Burkart MD. Manipulating fatty acid biosynthesis in microalgae for biofuel through protein-protein interactions. *PLoS One*. 2012;7(9):e42949.
35. Heath RJ, Rock CO. Inhibition of ketoacyl-acyl carrier protein synthase III (*FabH*) by acyl-acyl carrier protein in *Escherichia coli*. *J Biol Chem*. 1996;271(18):10996–1000.
36. Lin H, Fang L, Low CS, Chow Y, Lee YK. Occurrence of glycerol uptake in *Dunaliella tertiolecta* under hyperosmotic stress. *FEBS J*. 2013;280(4):1064–72.
37. Kindle KL. High-frequency nuclear transformation of *Chlamydomonas reinhardtii*. *Proc Natl Acad Sci USA*. 1990;87(3):1228–32.
38. Christie W. Lipid analysis: isolation, separation, identification, and structural analysis of lipids. Ayr: Oily Press. ISBN 0-9531949-5-7; 2003.
39. Lee S-Y, Kim S-H, Hyun S-H, Suh HW, Hong S-J, Cho B-K, et al. Fatty acids and global metabolites profiling of *Dunaliella tertiolecta* by shifting culture conditions to nitrate deficiency and high light at different growth phases. *Process Biochem*. 2014;49(6):996–1004.
40. Liu J, Sun Z, Zhong Y, Huang J, Hu Q, Chen F. Stearoyl-acyl carrier protein desaturase gene from the oleaginous microalga *Chlorella zofingiensis*: cloning, characterization and transcriptional analysis. *Planta*. 2012;236(6):1665–76.
41. Rumin J, Bonnefond H, Saint-Jean B, Rouxel C, Sciandra A, Bernard O, et al. The use of fluorescent Nile red and BODIPY for lipid measurement in microalgae. *Biotechnol Biofuels*. 2015;8(1):42.
42. Chen M, Tang H, Ma H, Holland TC, Ng KS, Salley SO. Effect of nutrients on growth and lipid accumulation in the green algae *Dunaliella tertiolecta*. *Bioresour Technol*. 2011;102(2):1649–55.
43. Shoaf WT, Lium BW. Improved extraction of chlorophyll a and b from algae using dimethyl sulfoxide. *Limnol Oceanogr*. 1976;21(6):926–8.

Submit your next manuscript to BioMed Central
and we will help you at every step:

- We accept pre-submission inquiries
- Our selector tool helps you to find the most relevant journal
- We provide round the clock customer support
- Convenient online submission
- Thorough peer review
- Inclusion in PubMed and all major indexing services
- Maximum visibility for your research

Submit your manuscript at
www.biomedcentral.com/submit

